Int J Thermophys (2015) 36:3255–3271
DOI 10.1007/s10765-015-1970-8

Thermal-Conductivity Measurement of Thermoelectric Materials Using 3ω Method

O. Hahtela[1] · M. Ruoho[2] · E. Mykkänen[1] · K. Ojasalo[1] · J. Nissilä[1] · A. Manninen[1] · M. Heinonen[1]

Received: 14 June 2013 / Accepted: 19 August 2015 / Published online: 4 September 2015

Abstract In this work, a measurement system for high-temperature thermal-conductivity measurements has been designed, constructed, and characterized. The system is based on the 3ω method which is an ac technique suitable for both bulk and thin-film samples. The thermal-conductivity measurements were performed in a horizontal three-zone tube furnace whose sample space can be evacuated to vacuum or alternatively a protective argon gas environment can be applied to prevent undesired oxidation and contamination of the sample material. The system was tested with several dielectric, semiconductor, and metal bulk samples from room temperature up to 725 K. The test materials were chosen so that the thermal-conductivity values covered a wide range from $0.37\,\mathrm{W\cdot m^{-1}\cdot K^{-1}}$ to $150\,\mathrm{W\cdot m^{-1}\cdot K^{-1}}$. An uncertainty analysis for the thermal-conductivity measurements was carried out. The measurement accuracy is mainly limited by the determination of the third harmonic of the voltage over the resistive metal heater strip that is used for heating the sample. A typical relative measurement uncertainty in the thermal-conductivity measurements was between 5 % and 8 % ($k = 2$). An extension of the 3ω method was also implemented in which the metal heater strip is first deposited on a transferable Kapton foil. Utilizing such a prefabricated sensor allows for faster measurements of the samples as there is no need to deposit a heater strip on each new sample.

卧式三区管式炉

Keywords 3ω method · Thermal conductivity · Thermoelectric

✉ O. Hahtela
ossi.hahtela@vtt.fi

1 VTT Technical Research Centre of Finland, Centre for Metrology (MIKES), Espoo, Finland

2 Department of Micro- and Nanosciences, Aalto University, Espoo, Finland

1 Introduction

Energy efficiency and sustainable energy sources are of great importance in developing modern and future technologies. Different kinds of energy harvesting processes, such as thermoelectricity, have gained increasing interest during recent years. Temperature gradients in thermoelectric materials create an electrical potential across the material which can be utilized for generating electrical power from wasted heat that is abundant in most human-related activities. Therefore, thermoelectric devices offer extensive possibilities to improve energy efficiency, reduce emissions, and reduce dependence of batteries and also cut operating costs of devices and processes.

The performance of thermoelectric devices is typically limited by the available materials. The efficiency of a thermoelectric material can be described with a dimensionless figure of merit ZT which is defined as

$$ZT = \frac{S^2 \sigma T}{\lambda}, \tag{1}$$

where S is the Seebeck coefficient, σ is the electrical conductivity, T is the absolute temperature, and λ is the thermal conductivity. Improving the ZT of traditional semiconducting thermoelectric materials, e.g., by doping, has limitations due to the interdependence of the parameters S, σ, and λ in bulk materials. However, nanotechnologies such as exploiting of thin films, nanowires, and nanopowders offer possibilities to enhance the energy conversion efficiency as the key material parameters can be tailored more individually by nanostructuring the materials. Nanostructuring can be utilized for achieving lower thermal-conductivity values than those of bulk materials because the grain boundaries, impurities, defects, and film interfaces will induce additional phonon scattering [1]. Besides tailoring the properties of the existing thermoelectric materials for enhancing the ZT, novel sustainable thermoelectric materials are also desired, e.g., to replace widely used tellurium alloys (Bi_2Te_3, Sb_2Te_3, and PbTe) which are expensive, scarce, and potentially hazardous to the environment. However, the lack of accurate and standardized measurement methods has hindered the development and reliable comparison of new thermoelectric materials.

The thermal conductivity of potential thermoelectric materials is preferably very low, on the order of 1 $W{\cdot}m^{-1}{\cdot}K^{-1}$, which makes an accurate determination of the thermal conductivity difficult especially when using traditional steady-state techniques at high temperatures [2]. The 3ω method was developed for the thermal-conductivity measurement of isotropic bulk materials by Cahill in the late 1980s [3] and has since been extensively used to measure thermal properties of a wide variety of materials. Besides measuring the thermal conductivity of solid materials, extensions of this method has also been used for liquids [4–6] and gases [7,8]. The 3ω method is an ac technique that is especially convenient in measurements that involve samples with small features or volume such as thin films [9–13], superlattice materials [14], nanowires [15], and nanotubes [16]. Due to the small volume that is heated during the measurement, the 3ω technique allows for relatively fast measurements and also the heat losses by radiation or through the substrate and wiring are of small importance [3].

In this paper we describe the design, operating principles, and testing of a measurement setup based on the 3ω method for determining the thermal conductivity of bulk materials from room temperature up to 725 K. We also present an uncertainty analysis for the 3ω measurements which validates our thermal-conductivity measurements.

2 Theory

In the 3ω method, a thin metal strip whose resistance depends on temperature is deposited on a dielectric sample (Fig. 1a). If the sample material is electrically conductive, an additional insulating layer is required between the metal heater strip and the sample to prevent the current leakage. The metal strip serves both as a heater and a thermometer. Typically, the geometry of the metal strip is chosen to be sufficiently thin, narrow, and long so that it can be considered as a line heater. A small sinusoidal electric current at angular frequency 1ω applied through the strip makes the temperature of the strip to oscillate at 2ω due to Joule heating. The heat diffuses into the sample underneath the heater strip, and the thermal penetration depth, $|q^{-1}|$, of the thermal waves depends on the applied frequency as

$$\left|\frac{1}{q}\right| = \sqrt{\frac{1}{2\omega}\frac{\lambda}{\rho C_V}}, \tag{2}$$

where ρ is the density and C_V is the specific heat of the sample material. The amplitude of the induced temperature oscillations depends on the heating power, geometry of the heater strip, and thermophysical properties, including the thermal conductivity, of the sample material. If the thermal penetration depth is large compared to the metal strip width, a linearized approximation for the complex temperature oscillation $\Delta T(\omega)$ is obtained as [3]

$$\Delta T\,(\omega) = \frac{P}{\pi l \lambda}\left[-\frac{1}{2}\ln(2\omega) + \frac{1}{2}\ln\frac{\lambda}{\rho C_V b^2} + \eta - \mathrm{i}\frac{\pi}{4}\right], \tag{3}$$

where P is the heating power, l is the length of the metal heater strip, b is the half-width of the metal strip, η is a constant, and i is the imaginary unit. This analytical model also assumes that the thermal penetration depth is smaller than the thickness of the sample, and the thickness of the heater strip is so small that its influence on the heat conduction can be neglected. These requirements are relatively easily fulfilled with typical bulk samples and measurement configurations. Because the resistance of the metal heater strip depends on the temperature, the strip resistance oscillates at 2ω. Thus, the voltage drop over the strip has a 1ω component and a small 3ω component. By monitoring the 3ω component of the voltage, $V_{3\omega}$, over the metal strip, e.g., with a lock-in amplifier (Fig. 1b), one can measure the temperature oscillation as [3]

$$\Delta T\,(\omega) = 2\frac{\mathrm{d}T}{\mathrm{d}R_0}\frac{R_0}{V_{1\omega}}V_{3\omega}, \tag{4}$$

where R_0 is the average resistance of the metal strip and $V_{1\omega}$ is the voltage over the metal strip at 1ω. Combining Eqs. 3 and 4, one can determine the thermal conductivity from the slope of the real part of the temperature oscillations (or equivalently the real part of the $V_{3\omega}$) plotted as a function of the natural logarithm of the applied frequency. Thus, the thermal conductivity is given by the equation,

$$\lambda = \frac{S_{\mathrm{R}} V_{1\omega}^3}{4\pi l R_0^2 S_T}, \tag{5}$$

where $S_{\mathrm{R}} = \mathrm{d}R_0/\mathrm{d}T$ is the temperature dependence of the heater strip resistance and S_T is the experimentally determined slope of the real part of $V_{3\omega}$ measured as a function of $\ln(2\omega)$.

3 Experiment

3.1 Sample Preparation

Our typical heater strip design with four electrical contact pads is illustrated in Fig. 1a. The width of the heater line is $2b = 50\,\mu\mathrm{m}$ and the length is $l = 3.5\,\mathrm{mm}$. The deposition and patterning of an approximately 100 nm thick gold heater strip were carried out using electron beam evaporation through a stainless-steel shadow mask. An additional 10 nm thick layer of chromium was grown between the gold film and the sample to improve the adhesion. The film thicknesses were controlled using a quartz crystal microbalance (QCM) during the deposition. In this work, the thermal conductivities of several dielectric, semiconductor, and metal samples were measured. Different kinds of samples with different electrical and mechanical properties required the development of their own kinds of techniques to prepare the sample and metal

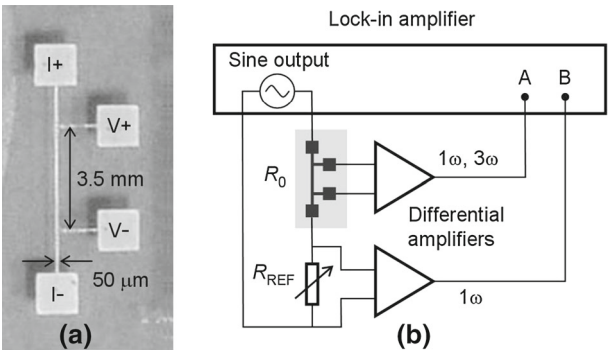

Fig. 1 (a) Photograph of a gold heater strip deposited on a borosilicate glass sample. The linewidth of the heater strip is $2b = 50\,\mu\mathrm{m}$. The heating ac current is supplied between the I+ and I− pads, and the $V_{3\omega}$ signal is measured between the $V+$ and $V-$ pads. The length of the heater strip between the voltage measurement pads is $l = 3.5\,\mathrm{mm}$. (b) Schematic diagram of the experimental measurement setup including the common mode subtraction. The small $V_{3\omega}$ voltage is detected by operating the lock-in amplifier in a differential mode which subtracts the dominant 1ω components over the heater strip and reference resistor

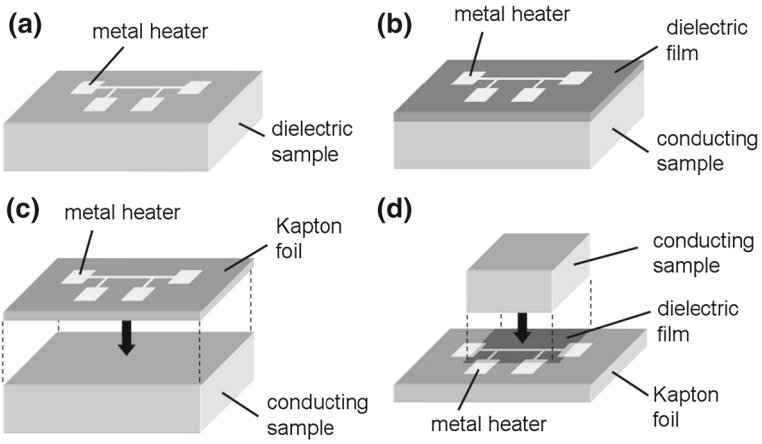

Fig. 2 (a) Metal heater strip can be deposited directly on a dielectric sample. (b) An electrically conductive sample requires an additional dielectric layer between the sample and heater strip. (c) The 3ω sensor can be prefabricated on a stand-alone Kapton foil which allows for the same transferable sensor to be used with several different samples. (d) An electrically conductive sample can also be attached on top of the prefabricated sensor if an additional dielectric layer is deposited on the heater strip

Table 1 Summary of the measured samples, measurement techniques, and sample preparation methods

	Sample material	Measurement technique[a]	Sample preparation
1	Borosilicate glass	a	Sample, Cr 10 nm, Au 100 nm
2	Borosilicate glass	c	Sample, DC 340[b], Kapton 50 μm, Cr 10 nm, Au 100 nm
3	Alumina	a	Sample, Cr 10 nm, Au 100 nm
4	Silicon	b	Sample, Al_2O_3 (ALD) 93 nm, Cr 10 nm, Au 100 nm
5	Bi_2Te_3, n-type	c	Sample, DC 340[b], Kapton 50 μm, Cr 10 nm, Au 100 nm
6	Bi_2Te_3, p-type	c	Sample, DC 340[b], Kapton 50 μm, Cr 10 nm, Au 100 nm
7	PbTe, No. 1	c	Sample, DC 340[b], Kapton 50 μm, Cr 10 nm, Au 100 nm
8	PbTe, No. 6	c	Sample, DC 340[b], Kapton 50 μm, Cr 10 nm, Au 100 nm
9	PbTe, No. 11	c	Sample, DC 340[b], Kapton 50 μm, Cr 10 nm, Au 100 nm
10	ISOTAN	d	Kapton substrate 125 μm, Cr 10 nm, Au 100 nm, Al_2O_3 (ALD) 135 nm, DC 340[b], sample

[a] Letter refers to the measurement method as indicated in Fig. 2
[b] Thermal paste (Dow Corning 340) was used to attach the sample and to improve thermal contact

heater strip configuration for the 3ω measurements (Fig. 2). The measured samples and the corresponding preparation techniques are listed in Table 1.

In the simplest case, the metal heater strip can be deposited directly on a dielectric sample (Fig. 2a). However, thermoelectric materials are typically semiconductors and they require an additional dielectric layer deposited between the sample and metal heater strip to prevent current leakage (Fig. 2b). If the thickness of the dielectric layer is much smaller than the width of the heater, the heat flow in the dielectric layer is mainly one-dimensional in the cross-plane direction. This will induce a frequency-

independent temperature drop across the dielectric film but no change in the slope of the temperature oscillation curve [9]. Therefore, an additional thin dielectric layer will not change the calculation of the thermal conductivity as presented in Eq. 5. The deposition of the additional dielectric layer such as SiN, SiO_2, or Al_2O_3 is relatively straightforward with many sample materials using, e.g., chemical vapor deposition (CVD), atomic layer deposition (ALD), and sputtering techniques. For example in this work, we used the ALD technique for depositing an isolating Al_2O_3 layer on a silicon sample.

The aforementioned deposition techniques do not necessarily work completely flawlessly with all sample materials, or they require special treatments of the sample surface. The adhesion of the dielectric material to the substrate may be poor causing stripping of the dielectric layer, or remaining pin holes may cause current leakage. In some cases it is also desired that the sample stays intact without the permanently deposited heater strip or dielectric layer. Therefore, some samples in this work were measured using a technique that was introduced by Jacquot et al. [17]. In this method, the metal heater strip is first deposited on a stand-alone Kapton foil (Fig. 2c) which serves both as a support membrane for the thin-film heater strip and as a dielectric layer. The Kapton foil is then attached to the sample surface, e.g., by using a thin layer of silicone-based thermal paste. A typical thickness of the thermal paste layer applied in this work was about 20 μm. Thermal paste, or equivalent, is also needed to improve the thermal contact between the sample and Kapton foil. Using such a prefabricated sensor allows for much faster and simpler measurement of new samples as there is no need to deposit a heater strip, and potentially an additional dielectric layer, on each individual sample but the same transferable sensor can be used for measuring several samples. The thickness of the Kapton film was the same 50 μm as the width of the metal heater strip. Ideally, the dielectric layer should be thin compared to the heater strip width. In addition, at higher measurement frequencies, the thermal penetration depth becomes so small that the heating effect takes place only in the Kapton film instead of the sample (see Fig. 5). However, by selecting low enough measurement frequencies, we were able to verify the applicability of this method in practice. We measured the thermal conductivity of borosilicate glass by both directly depositing the metal heater strip on the glass and utilizing the Kapton film method. In both cases, the measured thermal-conductivity values were equivalent within the uncertainty of the measurement as can be seen in Fig. 6. A disadvantage of using a Kapton film is that it does not tolerate very high temperatures. The highest temperature in our measurements utilizing a prefabricated Kapton sensor was about 415 K.

In order to reduce the possible contribution of the Kapton film to the measured thermal conductivity, we developed an extension of the Kapton film method (Fig. 2d). In this technique, an isolating 135 nm thick Al_2O_3 layer was deposited using the ALD technique on the same side of the Kapton film as the Au heater. The Al_2O_3 layer was patterned with a mask so that it covers only the heater line leaving the electrical contact pads free. Again, a thin layer of thermal paste is used to attach a conductive sample on top of the Al_2O_3 layer and to improve thermal contact. It should be noted that this method is suitable only for those sample materials that have a much larger thermal conductivity than that of Kapton. This ensures that most of the applied heating

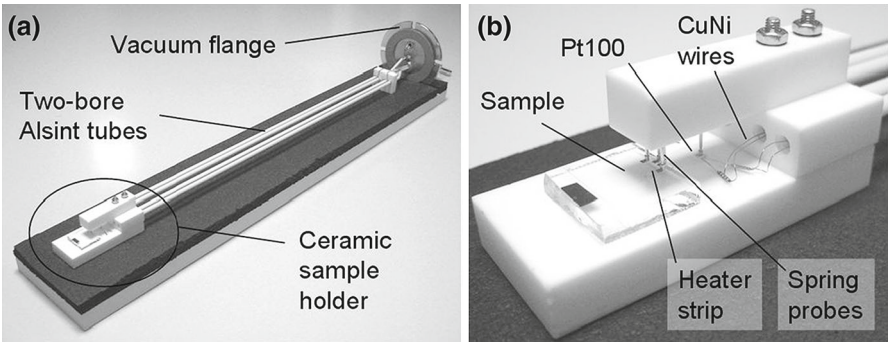

Fig. 3 (a) Measurement probe for the high-temperature thermal-conductivity measurements. The measurements are carried out in a horizontal tube furnace in ambient air, vacuum, or in protective argon gas environment. (b) Ceramic sample holder with a borosilicate glass sample. Spring probes are used to provide electrical contacts to the heater strip pads and to hold the sample in place. An additional Pt100 sensor monitors the temperature of the sample holder

diffuses into the sample material instead of the Kapton film which would distort the measurement.

3.2 Experimental Setup

Figure 3a shows the probe that was constructed for the high-temperature thermal-conductivity measurements. The sample holder (Fig. 3b) is fabricated from machinable
马克陶瓷 Macor ceramic. CuNi measurement wires with a diameter of 100 μm are conducted through two-bore Alsint tubes. Au-plated BeCu spring probes mounted to the ends of CuNi wires are used for providing electrical contact to the four measurement pads of the heater strip. The spring probes also hold the sample in place during the measurements. An additional Pt100 thermometer is used to monitor the sample-holder temperature. The measurements were performed in a horizontal three-zone tube furnace which provides accurate and uniform temperature control. At each temperature point, the temperature of the furnace was let to stabilize for one hour before starting the 3ω measurements or when the Pt100 sensor indicated a stable temperature. The sample space can be evacuated to vacuum or alternatively a protective argon gas environment can be applied to prevent undesired oxidation of the sample material, especially at high temperatures. The strip resistance R_0 is measured with an Agilent 3458A digital multimeter (DMM) using the standard four-point measurement method. The temperature dependence of the heater-strip resistance is determined by measuring the strip resistance value at different temperatures (Fig. 4).

3.3 Detection of the Third Harmonic

The measurement scheme for the 3ω technique used in this work is shown in Fig. 1b. The oscillations in the metal heater-strip temperature are obtained from the measurement of the third harmonic of the voltage over the heater strip. The internal voltage

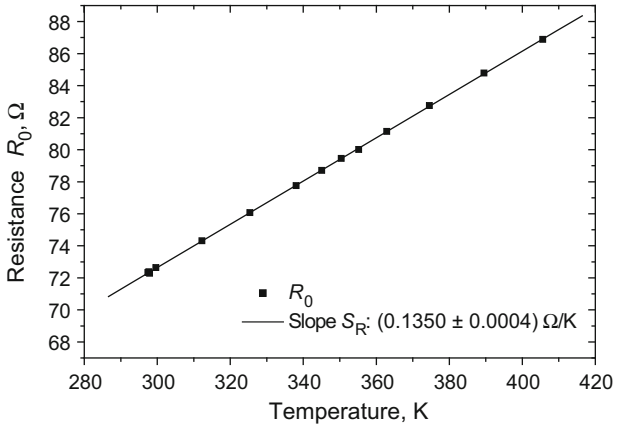

Fig. 4 The temperature dependence of the resistance of a Au-heater strip used for measuring the thermal conductivity of a Bi-doped PbTe bulk sample shows highly linear behavior in the temperature range from 300 K to 400 K

source of a Stanford Research Systems SR830 lock-in amplifier is used to provide an ac current through the metal strip at angular frequency ω. The heating power applied to the heater strip was typically between 1 mW and 10 mW. The voltage over the heater strip, which contains both 1ω and 3ω components, is obtained from a differential amplifier with unity gain. The 3ω component is typically about 1000 times smaller than the 1ω component. In order to get rid of the dominant 1ω voltage component, a common mode subtraction (CMS) technique [18] is used by adding a variable resistor R_{REF} in series with the heater strip. In addition, using the CMS makes it possible to employ a voltage-driven setup instead of an ideal current source [18]. The variable resistor is kept at a constant room temperature during the 3ω measurements, and R_{REF} is adjusted to be equal to R_0. Thus, the resulting voltage measured with the lock-in amplifier in a differential mode ideally contains only the 3ω component. The value of R_{REF} needs to be readjusted every time the sample temperature and, correspondingly, the value of R_0 is changed. The measurements are performed at such a range of frequencies that the amplitude of the real part of the temperature oscillations, or equivalently the $V_{3\omega}$, decreases linearly with $\ln(2\omega)$ (Fig. 5).

3.4 Measurement Uncertainty

The uncertainty analysis of the thermal-conductivity measurements based on the 3ω technique was carried out following the principles of the GUM [19] covering the experimental measurements according to Eq. 5. This analytical model developed by Cahill [3] includes approximations and assumptions that are not included in the uncertainty analysis but discussed and analyzed in detail elsewhere [18,20,21]. According to the uncertainty analysis, a typical relative uncertainty in our thermal-conductivity measurements performed for bulk samples in the temperature range from 300 K to

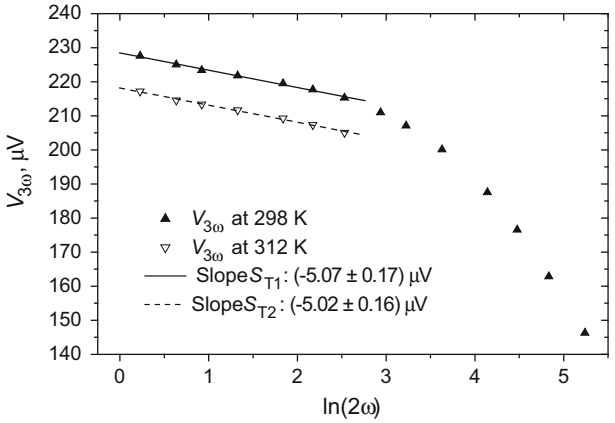

Fig. 5 Third harmonic voltages, $V_{3\omega}$, as a function of $\ln(2\omega)$ measured for a Bi-doped PbTe sample at temperatures of 298 K and 312 K. The frequency ranges in these two measurements were from 0.1 Hz to 15 Hz and from 0.1 Hz to 1 Hz, respectively. A 50 μm thick Kapton film was used as a dielectric layer. At high frequencies the thermal penetration depth becomes so small that the heating takes effectively at a place only in the Kapton film. The linear region at higher frequencies indicates a thermal conductivity of $0.37\,\mathrm{W\cdot m^{-1}\cdot K^{-1}}$ for Kapton at 298 K

725 K is between 5 % and 8 % ($k = 2$). The major uncertainty sources in the 3ω measurements were identified as follows:

$u(S_\mathrm{R})$ The temperature dependence of the metal heater-strip resistance is determined by measuring the resistance of the heater strip as the temperature of the sample is varied in a three-zone horizontal tube furnace. The resistance value is recorded using an Agilent 3458A digital multimeter, and the sample temperature is monitored with a Pt100 thermometer chip attached to the sample holder. Because we are interested in the temperature dependence of the resistance (i.e., $S_\mathrm{R} = \mathrm{d}R_0/\mathrm{d}T$), the stability and linearity of the resistance and temperature values are more critical than the absolute accuracy of the measured values. The standard uncertainty of the temperature dependence, $u(S_\mathrm{R})$, is determined as an uncertainty of the slope in the linear regression fit (Fig. 4). This uncertainty component is determined individually for each sample and heater-strip combination.

$u(V_{1\omega})$ The rms voltage $V_{1\omega}$ at frequency ω over the heater strip determines the applied heating power together with the heater resistance R_0. The $V_{1\omega}$ is measured using the SR830 lock-in amplifier with a typical uncertainty better than 0.2 %.

$u(l)$ The length of the heater strip on a sample is determined by the sputtering mask geometry and it is verified afterward on the ready-made sample using optical microscopy. The uncertainty in the visual inspection of the strip length is estimated to be 25 μm.

$u(R_0)$ The resistance of the heater strip is measured using an Agilent 3458A digital multimeter. The accuracy of the resistance measurement in our 3ω measurement is limited by the stability and small drifts of the resistance value during

the measurement rather than the performance of the DMM. A typical standard uncertainty in the resistance measurement (with a nominal value of 100 Ω) during a measurement period of 15 min is about 0.01 Ω.

$u(S_T)$ The largest contribution to the total uncertainty in the thermal-conductivity measurement originates from the determination of the $V_{3\omega}$ signal at different frequencies and the resulting linear regression fit. Because we are interested only in the slope of the $V_{3\omega}$ versus $\ln(2\omega)$ curve, the stability and linearity of the $V_{3\omega}$ values during the measurement are more important than the absolute accuracy. The standard uncertainty is determined as an uncertainty of the slope in the linear regression fit (Fig. 5). This uncertainty component is determined individually for each thermal-conductivity measurement at each temperature point.

The parameters determining the thermal conductivity in Eq. 5 are expected to be uncorrelated and the combined uncertainty $u(\lambda)$ of the thermal-conductivity measurement can be written as

$$u(\lambda) = \sqrt{C_{S_R}^2 u^2(S_R) + C_{V_{1\omega}}^2 u^2(V_{1\omega}) + C_l^2 u^2(l) + C_{R_0}^2 u^2(R_0) + C_{S_T}^2 u^2(S_T)}, \tag{6}$$

where the sensitivity coefficients corresponding to the partial derivatives are

$$C_{S_R} = \frac{\partial \lambda}{\partial S_R} = \frac{V_{1\omega}^3}{4\pi l R_0^2 S_T} \tag{7}$$

$$C_{V_{1\omega}} = \frac{\partial \lambda}{\partial V_{1\omega}} = \frac{3 S_R V_{1\omega}^2}{4\pi l R_0^2 S_T} \tag{8}$$

$$C_l = \frac{\partial \lambda}{\partial l} = -\frac{S_R V_{1\omega}^3}{4\pi l^2 R_0^2 S_T} \tag{9}$$

$$C_{R_0} = \frac{\partial \lambda}{\partial R_0} = -\frac{2 S_R V_{1\omega}^3}{4\pi l R_0^3 S_T} \tag{10}$$

$$C_{S_T} = \frac{\partial \lambda}{\partial S_T} = -\frac{S_R V_{1\omega}^3}{4\pi l R_0^2 S_T^2}. \tag{11}$$

Table 2 shows an example of an uncertainty budget which is calculated for a Bi-doped PbTe bulk sample measured at a temperature of $T = 312$ K.

4 Results

4.1 Test of the Method

To test the validity of our 3ω measurements, we measured the thermal conductivity of three reference materials (borosilicate glass, alumina, and silicon) with known thermal-conductivity values at different temperatures. The validity of the method was

Table 2 Uncertainty budget for the thermal conductivity of Bi-doped PbTe measured at 312 K

Uncertainty source	Standard uncertainty	Probability distribution	Sensitivity coefficient	Contribution
$u(S_R)$	$3.580 \times 10^{-4}\ \Omega \cdot K^{-1}$	Normal	$-19.17\ W \cdot m^{-1} \cdot \Omega^{-1}$	$-0.0069\ W \cdot m^{-1} \cdot K^{-1}$
$u(V_{1\omega})$	1.732×10^{-4} V	Rectangular	$-27.15\ W \cdot m^{-1} \cdot K^{-1} \cdot V^{-1}$	$-0.0047\ W \cdot m^{-1} \cdot K^{-1}$
$u(l)$	1.443×10^{-5} m	Rectangular	$739.3\ W \cdot m^{-2} \cdot K^{-1}$	$0.0107\ W \cdot m^{-1} \cdot K^{-1}$
$u(R_0)$	$1.000 \times 10^{-2}\ \Omega$	Normal	$0.06964\ W \cdot m^{-1} \cdot K^{-1} \cdot \Omega^{-1}$	$0.0007\ W \cdot m^{-1} \cdot K^{-1}$
$u(S_T)$	1.562×10^{-7} V	Normal	$-515478\ W \cdot m^{-1} \cdot K^{-1} \cdot V^{-1}$	$-0.0805\ W \cdot m^{-1} \cdot K^{-1}$
		Combined uncertainty $u(\lambda)$: $(k = 1)$		$0.08\ W \cdot m^{-1} \cdot K^{-1}$
Thermal conductivity : $2.59\ W \cdot m^{-1} \cdot K^{-1}$		Expanded uncertainty $\boldsymbol{U}(\boldsymbol{\lambda})$: $(\boldsymbol{k} = 2)$		$0.16\ W \cdot m^{-1} \cdot K^{-1}$
		Relative expanded uncertainty: $(k = 2)$		6 %

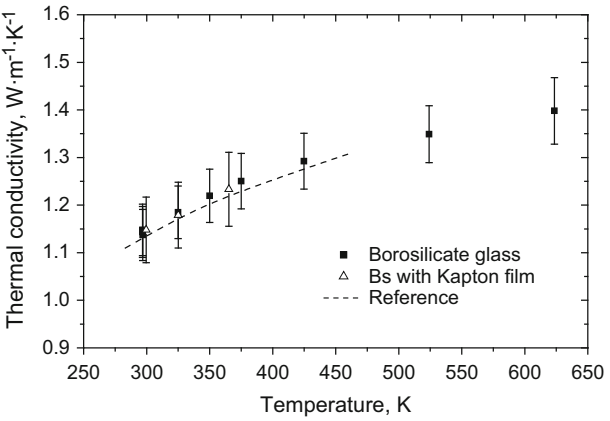

Fig. 6 Thermal conductivity of borosilicate glass was determined in the temperature range from 300 K to 625 K. *Error bars* indicate the expanded measurement uncertainty ($k = 2$) corresponding to an average relative uncertainty of 5 %. *Dashed line* shows the reference for the borosilicate glass from 283 K to 463 K [22]

also tested by measuring the same borosilicate glass sample in ambient air, argon gas, and in a vacuum environment, and there was no observable difference in the measured thermal-conductivity values due to the convection of the ambient gas within the uncertainty of the method. Figure 6 shows the measured thermal-conductivity values of a borosilicate glass bulk sample in the temperature range from 300 K to 625 K. The results are in good agreement with the reference values that were available from 283 K to 463 K [22]. The average relative measurement uncertainty was 5 % ($k = 2$). The size of the glass sample was 20 mm × 20 mm × 4 mm. In the first set of measurements, the Au-heater strip was deposited directly on the glass sample together with the 10 nm thick Cr adhesion layer. Then, the thermal conductivity was measured using the prefabricated Kapton film sensor. The results were similar in both measurements within the measurement uncertainty which validates the Kapton film method.

Bulk alumina (Al_2O_3) is widely used as a dielectric substrate material in different kinds of electronics applications, and it tolerates high temperatures. The thermal conductivity of an alumina sample was measured from 300 K to 725 K in argon gas (Fig. 7). The size of the alumina sample was 10 mm × 10 mm × 1 mm, and the heater strip was deposited directly on the sample. The measured values had an average relative uncertainty of 7 % ($k = 2$), and the results show good agreement with the values in [23].

Figure 8 shows the results of the thermal-conductivity measurements carried out with a piece of silicon which was cut from a 380 μm thick silicon wafer. Silicon is a semiconductor material, and therefore it requires an additional dielectric layer before depositing the metal heater strip. We used the ALD technique to deposit an electrically insulating 93 nm thick Al_2O_3 thin film on the silicon sample. It was noticed that there was a slightly increased variation in the measured thermal-conductivity values, and the measurement uncertainty was higher for silicon than for other materials measured in this work. The increased measurement uncertainty can be explained by the fact that, as the thermal conductivity of silicon is relatively high, the slope of the $V_{3\omega}$ versus

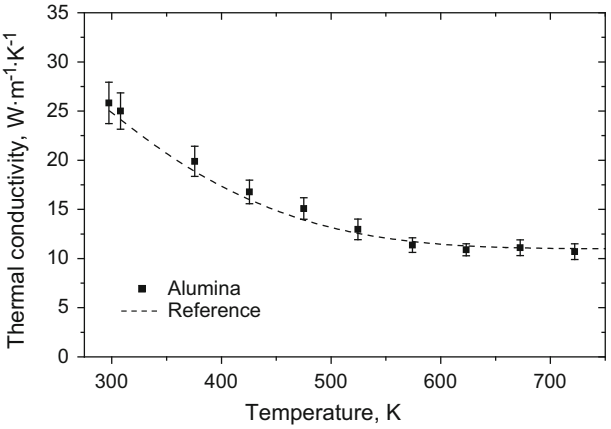

Fig. 7 Thermal conductivity of alumina bulk sample was measured from 300 K to 725 K with an average relative uncertainty of 7 % ($k = 2$). *Dashed line* shows the reference for alumina [23]

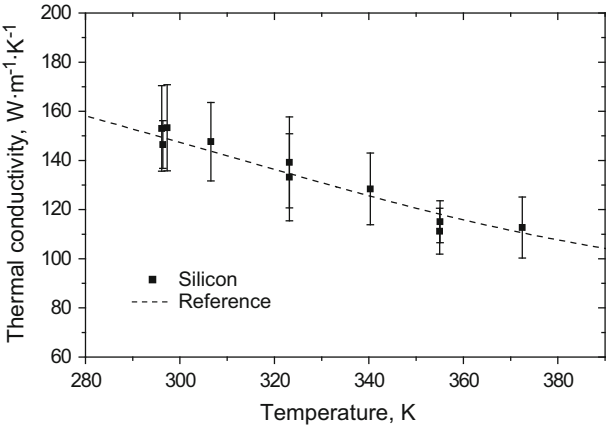

Fig. 8 Thermal conductivity of silicon was measured as a function of temperature. The average relative uncertainty was 10 % ($k = 2$). *Dashed line* shows the reference for pure silicon [24]

$\ln(2\omega)$ curve is almost flat and the determination of such a slope with good accuracy becomes more difficult.

4.2 Thermal Conductivity of Bismuth Telluride

After validating the measurement system with the known reference materials, we continued the thermal-conductivity measurements with thermoelectric materials. At present, bismuth telluride alloys are the most common bulk materials used in different kinds of thermoelectric applications. Figure 9 shows the measured thermal conductivity of an *n*-type Bi_2Te_3 and a *p*-type $Bi_{0.3}Sb_{1.7}Te_3$ sample. The samples were fabricated using the hot-pressing method, and the size of both samples was

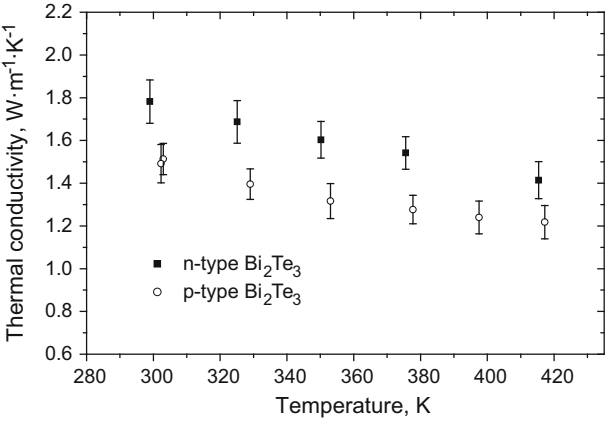

Fig. 9 Thermal conductivity of an *n*-type Bi_2Te_3 and a *p*-type $Bi_{0.3}Sb_{1.7}Te_3$ bulk samples measured in the temperature range from 300 K to 415 K. The average relative uncertainty in both measurements is 6 % ($k = 2$)

20 mm × 4 mm × 4 mm. The measurements were performed in ambient air and in the temperature range from 300 K to 415 K using the Kapton film method. The average relative measurement uncertainty for both samples was 6 % ($k = 2$). Accurate reference values for the thermal conductivity of such Bi_2Te_3 samples are not available because the thermal properties depend strongly on the fabrication process and exact chemical composition of the sample. In addition, it should be noted that, because the thermal conductivity of hot pressed bismuth telluride is anisotropic, the measured values for both *n*- and *p*-type bismuth telluride samples should be considered as effective thermal conductivities.

4.3 Thermal Conductivity of Bismuth-Doped Lead Telluride

Besides the bismuth telluride alloys, lead telluride alloys are also widely used thermoelectric materials. Figure 10 shows the measurement results for three Bi-doped PbTe samples originating from the same fabrication batch. The samples were fabricated using the spark plasma sintering (SPS) method, and the chemical composition of the material was $Pb_1Te_{0.85}Bi_{0.15}$. The size of the PbTe samples was 15 mm × 2.5 mm × 1.5 mm. The samples were measured in argon gas using the Kapton film method. According to the measurements, each of the three samples has a similar thermal conductivity in the temperature range from 300 K to 410 K. The average relative measurement uncertainty was 6 % ($k = 2$).

4.4 Thermal Conductivity of ISOTAN

The ISOTAN metal alloy (Cu55Ni44Mn1) has good thermal and mechanical stability at elevated temperatures and is thus a potential candidate to be used as a thermoelectric reference material. Figure 11 shows the measured thermal conductivity of ISOTAN as a

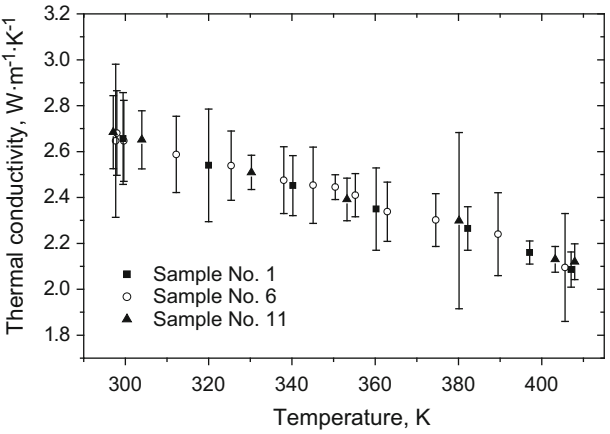

Fig. 10 Thermal conductivity of three Bi-doped PbTe bulk samples originating from the same fabrication batch was determined in the temperature range from 300 K to 410 K. Average relative uncertainty was 6 % ($k = 2$)

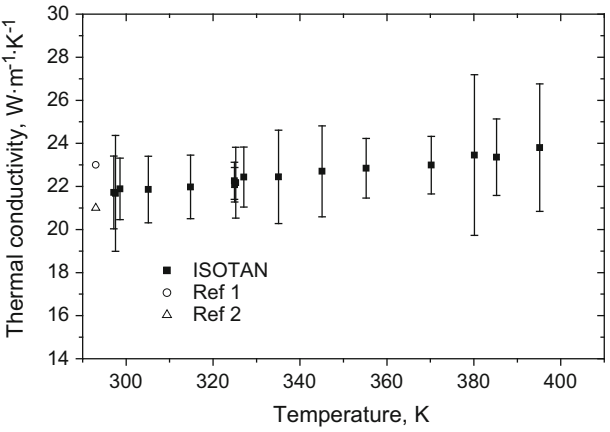

Fig. 11 Thermal conductivity of a 1 mm thick ISOTAN bulk sample was measured in the temperature range from 300 K to 400 K with an average relative uncertainty of 8 % ($k = 2$). Two slightly different reference values for ISOTAN at 293 K were found in the literature: 23 $W{\cdot}m^{-1}{\cdot}K^{-1}$ [25] and 21 $W{\cdot}m^{-1}{\cdot}K^{-1}$ [26]

function of temperature. The size of the ISOTAN sample was 10 mm × 4.5 mm × 1 mm. In this measurement, we used the extension of the Kapton film technique in which the Kapton film serves as a substrate for the heater strip, and an additional Al_2O_3 isolation layer is deposited on the metal heater strip using the ALD technique. The ISOTAN sample was mounted on top of the Al_2O_3 thin film using a thin layer of thermal paste. The measurements were performed in ambient air in the temperature range from 300 K to 400 K. The measured values agree, within experimental uncertainties, with the two reference values that were found in the literature [25,26].

5 Conclusion

A 3ω measurement system was successfully developed at MIKES for determining the thermal conductivity of bulk samples from room temperature to 725 K. After validating the system with known reference materials, it was utilized for measuring several thermoelectric samples. The thermal-conductivity values measured in this work covered a wide range from $0.37\,\mathrm{W\cdot m^{-1}\cdot K^{-1}}$ to $150\,\mathrm{W\cdot m^{-1}\cdot K^{-1}}$. We also implemented an extension of the 3ω method which includes a prefabricated sensor deposited on a stand-alone Kapton foil. Such a transferable sensor allows for faster and simpler thermal-conductivity measurements without the need to deposit the metal heater and potentially a dielectric layer on every new sample. It was demonstrated by measurements that the relatively thick Kapton film between the sample and heater has no significant influence on the thermal-conductivity measurement if the measurement frequency range is chosen properly. The thermal-conductivity values we obtained for the reference samples were in good agreement with the data found in the literature validating the eligibility of our measurements. A measurement uncertainty analysis was carried out showing that the relative uncertainty in our 3ω measurements is typically between 5 % and 8 % ($k = 2$) which is a good accuracy for measuring the thermal conductivity of materials at elevated temperatures. Such accurate and validated thermal-conductivity measurements are of great importance in developing and comparing new materials, e.g., for thermoelectric applications.

Acknowledgments This work has received funding from the European Union on the basis of Decision No 912/2009/EC. The research has been carried out in the framework of the European Metrology Research Programme Eng02 - Metrology for Energy Harvesting. The development of the sample preparation techniques was partly funded by the Academy of Finland Project Number 140009, Cleen Ltd. and TEKES (the Finnish Funding Agency for Technology and Innovation).

References

1. E.S. Toberer, L.L. Baranowski, C. Dames, Annu. Rev. Mater. Res. **42**, 179 (2012)
2. D.M. Rowe (ed.), *Thermoelectrics Handbook: Macro to Nano* (CRC Press, Boca Raton, FL, 2006)
3. D.G. Cahill, Rev. Sci. Instrum. **61**, 802 (1990)
4. I.K. Moon, Y.H. Jeong, Rev. Sci. Instrum. **67**, 29 (1996)
5. F. Chen, J. Shulman, Y. Xue, C.W. Chu, G.S. Nolas, Rev. Sci. Instrum. **75**, 4578 (2004)
6. S.-M. Lee, Rev. Sci. Instrum. **80**, 024901 (2009)
7. E. Yusibani, P.L. Woodfield, M. Fujii, K. Shinzato, X. Zhang, Y. Takata, Int. J. Thermophys. **30**, 397 (2009)
8. S. Gauthier, A. Giani, P. Combette, Sens. Actuators A **195**, 50 (2013)
9. D.G. Cahill, M. Katiyar, J.R. Abelson, Phys. Rev. B **50**, 6077 (1994)
10. S.-M. Lee, D.G. Cahill, J. Appl. Phys. **81**, 2590 (1997)
11. T. Yamane, N. Nagai, S.I. Katayama, M. Todoki, J. Appl. Phys. **91**, 9772 (2002)
12. A. Jain, K.E. Goodson, J. Heat Trans. **130**, 102402 (2008)
13. J. Alvarez-Quintana, J. Rodríguez-Viejo, Sens. Actuators A **142**, 232 (2008)
14. B. Shen, Z. Zeng, C. Lin, Z. Hu, Int. J. Therm. Sci. **66**, 19 (2013)
15. A. Holtzman, E. Shapira, Y. Selzer, Nanotechnology **23**, 495711 (2012)
16. J. Hu, A.A. Padilla, J. Xu, T.S. Fisher, K.E. Goodson, J. Heat Trans. **128**, 1109 (2006)
17. A. Jacquot, F. Vollmer, B. Bayer, M. Jaegle, D.G. Ebling, H. Böttner, J. Electron. Mater. **39**, 1621 (2010)
18. J. Kimling, S. Martens, K. Nielsch, Rev. Sci. Instrum. **82**, 074903 (2011)

19. JCGM 100:2008, Evaluation of measurement data—guide to the expression of uncertainty in measurement, 1st edn. (2008)
20. A. Jacquot, B. Lenoir, A. Dauscher, M. Stölzer, J. Meusel, J. Appl. Phys. **91**, 4733 (2002)
21. H. Wang, M. Sen, Int. J. Heat Mass Trans. **52**, 2102 (2009)
22. UQG Ltd., SCHOTT BOROFLOAT thermal properties, http://www.uqgoptics.com/materials_commercial_schott_borofloat.aspx. Accessed 29 November 2013
23. NTK Technologies Inc., Comparison of ceramic materials, http://www.ntktech.com/AlN/ALN%20for%20web.pdf. p. 8. Accessed 29 November 2013
24. eFunda Inc., Thermal conductivity of silicon, http://www.efunda.com/materials/elements/TC_Table.cfm?Element_ID=Si. Accessed 29 November 2013
25. Isabellenhütte Heusler GmbH & Co., ISOTAN properties and application notes, http://www.isabellenhuette.de/fileadmin/content/widerstandslegierungen/ISOTAN-ISABELLENHUETTE-R.pdf. Accessed 29 November 2013
26. Ferd. Wagner GmbH, ISOTAN technical data sheet, http://www.zapp.com/fileadmin/downloads/01-Produkte/Datenblaetter-Praezisionsprofile-Ferd-Wagner/Werkstoffdatenbl%C3%A4tter%20englisch/engl_isotan%20Cu%20Ni44.pdf. Accessed 29 November 2013